

Supporting Information

Synthesis, Structure, and Superconductivity of B-site Doped Perovskite Bismuth Lead Oxide with Indium

Xiande Zheng^b, Lei Zhang^a, Xiaoge Wang^a, Yiguo Qing^c, Jie Chen^f, Yaoda Wu^f, Sihao Deng^f, Lunhua He^{d,e,f}, Fuhui Liao^a, Yan Wang^a, Jinling Geng^a, Junliang Sun^a, Guobao Li^{a*}, Laijun Liu^{b*}, Jianhua Lin^{a*}

^aBeijing National Laboratory for Molecular Sciences, State Key Laboratory of Rare Earth Materials Chemistry and Applications, College of Chemistry and Molecular Engineering, Peking University, Beijing 100871, People's Republic of China

^bCollege of Materials Science and Engineering, Guilin University of Technology, Guilin 541004, People's Republic of China

^cBeijing No. 80 High School, Beijing 100102, People's Republic of China

^dBeijing National Laboratory for Condensed Matter Physics, Institute of Physics, Chinese Academy of Sciences, Beijing 100190, People's Republic of China

^eSongshan Lake Materials Laboratory, Dongguan 523808, People's Republic of China

^fSpallation Neutron Source Science Center, Dongguan, 523803, People's Republic of China

Email: liguobao@pku.edu.cn, and jhlin@pku.edu.cn; Tel: (8610)62750342, Fax: (8610)62753541.

Contents

| | |
|---|----|
| 1. The refinement details of the X-ray and neutron diffraction data of In1, In5, In9, and BaBiO _{3-δ} using <i>P</i> -1 space group..... | 2 |
| 2. The refinement details of the X-ray diffraction data of In2, In3, In4, In6, In7, In8, In10, In11, In12, and In13 | 3 |
| 3. Temperature-dependent resistance of Ba(Bi _{0.25} Pb _{0.75}) _{1-x} In _x O _{3-δ} | 10 |

1. The refinement details of the X-ray and neutron diffraction data of In1, In5, In9, and BaBiO_{3-δ} using *P*-1 space group.

Table S1. Rietveld refinement details of the X-ray and neutron diffraction data for BaBi_{0.25}Pb_{0.75}O_{3-δ} (In1) in space group *P*-1.

| Lattice parameter | a=6.0632(2)Å, b=6.0573(3)Å, c=6.0669(3)Å, α=60.24(1)°, β=59.93(2)°, γ=60.03(2)°. | | |
|-----------------------|---|-------------|------------------|
| Atom | x, y, z | Occupancy | U _{iso} |
| Ba1 | 0.2562(1), 0.2583(2), 0.2410(1) | 1.000 | 0.0038(4) |
| Bi1/Pb1 | 0.0000, 0.0000, 0.0000 | 0.250/0.750 | 0.0029(3) |
| Bi2/Pb2 | 0.5000, 0.5000, 0.5000 | 0.250/0.750 | 0.0047(4) |
| O1 | 0.3050(3), 0.1870(3), 0.7420(4) | 0.986(4) | 0.0083(4) |
| O2 | 0.7556(3), 0.2753(3), 0.2265(2) | 0.986(4) | 0.0103(5) |
| O3 | 0.2283(3), 0.7494(4), 0.2739(3) | 0.986(4) | 0.0074(3) |
| R factor ^a | Rx wp=0.049, Rx p=0.032; Rn wp=0.079, Rn p=0.060 | | |

^aRx wp, Rx p; Rn wp, Rn p are the R factors of the whole patterns and the peaks for X-ray (x) and neutron (n) diffraction data, respectively.

Table S2. Rietveld refinement details of the X-ray and neutron diffraction data for BaBi_{0.24}Pb_{0.72}In_{0.04}O_{3-δ} (In5) in space group *P*-1.

| Lattice parameter | a=6.0657(3)Å, b=6.0582(2)Å, c=6.0640(3)Å, α=60.20(2)°, β=59.86(1)°, γ=60.06(2)°. | | |
|-----------------------|---|-------------------|------------------|
| Atom | x, y, z | Occupancy | U _{iso} |
| Ba1 | 0.2510(2), 0.2596(2), 0.2403(1) | 1.000 | 0.0091(5) |
| Bi/Pb/In1 | 0.0000, 0.0000, 0.0000 | 0.240/0.720/0.040 | 0.0057(3) |
| Bi/Pb/In2 | 0.5000, 0.5000, 0.5000 | 0.240/0.720/0.040 | 0.0061(4) |
| O1 | 0.2791(3), -0.2055(3), 0.7092(4) | 0.986(5) | 0.0169(5) |
| O2 | 0.7634(3), 0.7299(3), 0.2364(2) | 0.985(4) | 0.0100(5) |
| O3 | 0.2268(3), 0.7442(4), 0.2787(3) | 0.987(6) | 0.0159(6) |
| R factor ^a | Rx wp=0.040, Rx p=0.028; Rn wp=0.059, Rn p=0.045 | | |

^aRx wp, Rx p; Rn wp, Rn p are the R factors of the whole patterns and the peaks for X-ray (x) and neutron (n) diffraction data, respectively.

Table S3. Rietveld refinement details of the X-ray and neutron diffraction data for BaBi_{0.23}Pb_{0.69}In_{0.08}O_{3-δ} (In9) in space group *P*-1.

| Lattice parameter | a=6.0646(2)Å, b=6.0599(3)Å, c=6.0603(3)Å, α=60.26(1)°, β=59.82(2)°, γ=60.07(2)°. | | |
|-----------------------|---|-------------------|------------------|
| Atom | x, y, z | Occupancy | U _{iso} |
| Ba1 | 0.2430(1), 0.2589(2), 0.2444(1) | 1.000 | 0.0082(4) |
| Bi/Pb/In1 | 0.0000, 0.0000, 0.0000 | 0.230/0.690/0.080 | 0.0063(3) |
| Bi/Pb/In2 | 0.5000, 0.5000, 0.5000 | 0.230/0.690/0.080 | 0.0063(3) |
| O1 | 0.2524(3), -0.2152(3), 0.7165(4) | 0.982(5) | 0.0124(4) |
| O2 | 0.7605(3), 0.7377(3), 0.2383(2) | 0.983(4) | 0.0116(3) |
| O3 | 0.2733(3), 0.7004(4), 0.2282(3) | 0.983(4) | 0.0201(5) |
| R factor ^a | Rx wp=0.045, Rx p=0.030; Rn wp=0.063, Rn p=0.050 | | |

^aRx wp, Rx p; Rn wp, Rn p are the R factors of the whole patterns and the peaks for X-ray (x) and neutron (n) diffraction data, respectively.

Table S4. Rietveld refinement details of the X-ray and neutron diffraction data for BaBiO_{3-δ} in space group *P*-1.

| Lattice parameter | a=6.1406(3)Å, b=6.1865(2)Å, c=6.1437(2)Å, α=59.90(1)°, β=59.98(2)°, γ=59.87(2)°. | | |
|-----------------------|---|-----------|------------------|
| Atom | x, y, z | Occupancy | U _{iso} |
| Ba1 | 0.2519(2), 0.2532(2), 0.2454(1) | 1.000 | 0.0090(4) |
| Bi1 | 0.0000, 0.0000, 0.0000 | 1.000 | 0.0068(3) |
| Bi2 | 0.5000, 0.5000, 0.5000 | 1.000 | 0.0068(3) |
| O1 | 0.2206(3), 0.3012(2), 0.7038(4) | 1.000 | 0.0185(5) |
| O2 | 0.7124(3), 0.2815(3), 0.2310(2) | 1.000 | 0.0182(3) |
| O3 | 0.2710(4), 0.8032(3), 0.2480(3) | 1.000 | 0.0171(4) |
| R factor ^a | Rx wp=0.064, Rx p=0.047; Rn wp=0.074, Rn p=0.057 | | |

^aR_x wp, R_x p; R_n wp, R_n p are the R factors of the whole patterns and the peaks for X-ray (x) and neutron (n) diffraction data, respectively.

2. The refinement details of the X-ray diffraction data of In2, In3, In4, In6, In7, In8, In10, In11, In12, and In13.

The Powder X-ray powder diffraction data collected at room temperature for In2, In3, In4, In6, In7, In8, In10, In11, In12 and In13 are refined using GSAS software. The refinement details listed in Table S5, S6, S7, S8. The corresponding Rietveld plots are shown in Fig. S1, S2, ..., S10.

Table S5 Rietveld refinement details of the X-ray diffraction data for In2, In3 and In4 in *P1*.

| | In2 | In3 | In4 |
|--------------------------|--|--|--|
| Lattice parameter | a=6.0677(2)Å, b=6.0543(3)Å, c=6.0679(3)Å, $\alpha=60.18(1)^\circ$, $\beta=59.87(2)^\circ$, $\gamma=60.08(2)^\circ$ | a=6.0682(3) Å, b=6.0545 (3)Å, c=6.0644(3)Å, $\alpha=60.22(1)^\circ$, $\beta=59.89(2)^\circ$, $\gamma=60.07(2)^\circ$ | a=6.0673(1)Å, b=6.0545(3)Å, c=6.0645(2)Å, $\alpha=60.21(3)^\circ$, $\beta=59.89(2)^\circ$, $\gamma=60.07(1)^\circ$ |
| Atom | x, y, z | x, y, z | x, y, z |
| Ba1 ^a | 0.2416(1), 0.2656(2), 0.2481(1) | 0.2564(1), 0.2611(2), 0.2414(1) | 0.2515(1), 0.2649(1), 0.2398(1) |
| Ba2 ^a | 0.7446(3), 0.7666(2), 0.7479(2) | 0.7512(2), 0.7651(3), 0.7447(3) | 0.7532(3), 0.7644(2), 0.7412(3) |
| Bi1/Pb1/In1 ^b | 0.0000, 0.0000, 0.0000 | 0.0000, 0.0000, 0.0000 | 0.0000, 0.0000, 0.0000 |
| Bi2/Pb2/In2 ^b | 0.4995(2), 0.4964(2), 0.5029(2) | 0.4976(2), 0.4979(2), 0.5038(3) | 0.5033(1), 0.4948(2), 0.5037(3) |
| O1 ^c | 0.2617(1), -0.7476(2), 0.7061(3) | 0.2511(1), -0.7595(3), 0.6935(3) | 0.2538(1), -0.7538(3), 0.7014(1) |
| O2 ^c | 0.8352(3), 0.6858(2), 0.1793(1) | 0.8426(3), 0.6454(2), 0.2141(1) | 0.8414(2), 0.6540(2), 0.2155(1) |
| O3 ^c | 0.7521(2), 0.2470(3), 0.2398(1) | 0.7355(3), 0.2274(1), 0.2735(2) | 0.7177(3), 0.2541(1), 0.2504(1) |
| O4 ^c | 0.2432(1), 0.7217(1), 0.7433(1) | 0.2268(1), 0.7142(3), 0.7871(3) | 0.2532(3), 0.7020(3), 0.7816(3) |
| O5 ^c | 0.2176(1), 0.7480(2), 0.3053(1) | 0.1918(1), 0.7488(3), 0.3149(2) | 0.1959(2), 0.7488(3), 0.3070(1) |
| O6 ^c | 0.7621(2), 0.2258(1), 0.7946(1) | 0.7409(3), 0.2704(2), 0.7618(3) | 0.7278(3), 0.2285(1), 0.7926(3) |
| R factor ^d | R _{wp} =0.0613, R _p =0.0365 | R _{wp} =0.0433, R _p =0.0288 | R _{wp} =0.0424, R _p =0.0286 |

^aThe occupancies of Ba1 and Ba2 are 1.0000 for In2, In3 and In4.

^bThe occupancies of Bi1/Pb1/In1 and Bi2/Pb2/In2 are 0.2475/0.7425/0.0100 for In2, 0.2450/0.7350/0.0200 for In3, and 0.2425/0.7275/0.0300 for In4.

^cThe occupancies of O1, O2, O3, O4, O5, and O6 are 1.0000, 1.0000, 1.0000, 1.0000, 1.0000, 1.0000 for In2, In3 and In4.

^dR_p is sum(|I₀-I_C|)/sum(I₀), and R_{wp} is weighted R factors for X-ray diffraction data.

Table S6 Rietveld refinement details of the X-ray diffraction data for In6, In7 and In8 in *P1*.

| | In6 | In7 | In8 |
|--------------------------|---|---|--|
| Lattice parameter | a=6.0673(1)Å, b=6.0599(3)Å, c=6.0609(3)Å, $\alpha=60.20(1)^\circ$, $\beta=59.84(2)^\circ$, $\gamma=60.07 (2)^\circ$ | a=6.0679(3) Å, b=6.0587 (3)Å, c= 6.0591(3)Å, $\alpha=60.24(1)^\circ$, $\beta=59.84(2)^\circ$, $\gamma=60.07(2)^\circ$ | a=6.0647(1)Å, b=6.0600(3)Å, c=6.0624(2)Å, $\alpha=60.23(3)^\circ$, $\beta=59.82(2)^\circ$, $\gamma=60.06(1)^\circ$ |
| Atom | x, y, z | x, y, z | x, y, z |
| Ba1 ^a | 0.2483(1), 0.2661(2), 0.2414(1) | 0.2491(1), 0.2658(2), 0.2412(1) | 0.2495(1), 0.2654(2), 0.2416(1) |
| Ba2 ^a | 0.7494(3), 0.7663(3), 0.7413(3) | 0.7502(3), 0.7661(3), 0.7408(3) | 0.7508(3), 0.7655(3), 0.7425(3) |
| Bi1/Pb1/In1 ^b | 0.0000, 0.0000, 0.0000 | 0.0000, 0.0000, 0.0000 | 0.0000, 0.0000, 0.0000 |
| Bi2/Pb2/In2 ^b | 0.5049(2), 0.4945(2), 0.5030(2) | 0.5047(2), 0.4943(2), 0.5032(2) | 0.5036(2), 0.4950(2), 0.5035(2) |
| O1 ^c | 0.2599(1), -0.7678(3), 0.7035(3) | 0.2651(2), -0.7727(3), 0.6954(2) | 0.2443(1), -0.7596(3), 0.6818(3) |
| O2 ^c | 0.7935(3), 0.6932(2), 0.1647(1) | 0.8019(3), 0.6919(2), 0.1587(1) | 0.8355(3), 0.6308(2), 0.2201(3) |
| O3 ^c | 0.7535(3), 0.2542(1), | 0.7475(3), 0.2517(1), 0.2303(1) | 0.7277(3), 0.2460(1), 0.2382(1) |

| | | | |
|-----------------------|---|---|---|
| O4 ^c | 0.2302(2) 0.2371(1), 0.7362(3), 0.7567(3) | 0.2357(1), 0.7290(2), 0.7527(3) | 0.2194(1), 0.7414(3), 0.7467(3) |
| O5 ^c | 0.1826(1), 0.7709(3), 0.3171(2) | 0.1852(1), 0.7798(3), 0.3115(2) | 0.1949(1), 0.7529(3), 0.3239(3) |
| O6 ^c | 0.7191(3), 0.2368(1), 0.8064(3) | 0.7135(3), 0.2472(1), 0.7969(3) | 0.7351(3), 0.2232(1), 0.8176(3) |
| R factor ^d | R _{wp} =0.0514, R _p =0.0341 | R _{wp} =0.0452, R _p =0.0299 | R _{wp} =0.0410, R _p =0.0284 |

^aThe occupancies of Ba1 and Ba2 are 1.0000 for In6, In7 and In8.

^bThe occupancies of Bi1/Pb1/In1 and Bi2/Pb2/In2 are 0.2375/0.7125/0.0500 for In6, 0.2350/0.7050/0.0600 for In7, and 0.2325/0.6975/0.0700 for In8.

^cThe occupancies of O1, O2, O3, O4, O5, and O6 are 1.0000, 1.0000, 1.0000, 1.0000, 1.0000 for In6, In7 and In8.

^dR_p is sum(|I₀-I_C|)/sum(I₀), and R_{wp} is weighted R factors for X-ray diffraction data.

Table S7 Rietveld refinement details of the X-ray diffraction data for In10 and In11 in *P1*.

| | In10 | In11 |
|--------------------------|--|--|
| Lattice parameter | a=6.0598(2)Å, b=6.0624(3)Å, c=6.0652(3)Å, α =60.26(1) $^\circ$, β =59.79(2) $^\circ$, γ =60.03(2) $^\circ$ | a=6.0594(3) Å, b=6.0640 (3)Å, c=6.0625(3)Å, α =60.30(1) $^\circ$, β =59.76(2) $^\circ$, γ =60.04(2) $^\circ$ |
| Atom | x, y, z | x, y, z |
| Ba1 ^a | 0.2504(1), 0.2641(1), 0.2449(1) | 0.2492(1), 0.2648(1), 0.2439(1) |
| Ba2 ^a | 0.7485(3), 0.7656(3), 0.7481(3) | 0.7480(3), 0.7662(3), 0.7457(3) |
| Bi1/Pb1/In1 ^b | 0.0000, 0.0000, 0.0000 | 0.0000, 0.0000, 0.0000 |
| Bi2/Pb2/In2 ^b | 0.5047(2), 0.4949(2), 0.5014(2) | 0.5045(2), 0.4945(2), 0.5027(2) |
| O1 ^c | 0.2321(1), -0.7396(3), 0.6850(3) | 0.2543(1), -0.7599(3), 0.6954(2) |
| O2 ^c | 0.8459(3), 0.6327(2), 0.2359(1) | 0.8379(3), 0.6352(2), 0.2264(1) |
| O3 ^c | 0.7362(3), 0.2523(1), 0.2251(1) | 0.7360(3), 0.2557(1), 0.2274(1) |
| O4 ^c | 0.2336(1), 0.7477(3), 0.7213(3) | 0.2163(3), 0.7594(3), 0.7392(3) |
| O5 ^c | 0.2154(2), 0.7428(3), 0.3067(3) | 0.2045(1), 0.7606(3), 0.3127(2) |
| O6 ^c | 0.7451(3), 0.2155(1), 0.8014(3) | 0.7264(3), 0.2341(1), 0.8071(3) |
| R factor ^d | R _{wp} =0.0415, R _p =0.0282 | R _{wp} =0.0459, R _p =0.0316 |

^aThe occupancies of Ba1 and Ba2 are 1.0000 for In10 and In11.

^bThe occupancies of Bi1/Pb1/In1 and Bi2/Pb2/In2 are 0.2275/0.6825/0.0900 for In10 and 0.2250/0.6750/0.1000 for In11.

^cThe occupancies of O1, O2, O3, O4, O5, and O6 are 1.0000, 1.0000, 1.0000, 1.0000, 1.0000 for In10 and In11.

^dR_p is sum(|I₀-I_C|)/sum(I₀), and R_{wp} is weighted R factors for X-ray diffraction data.

Table S8 Rietveld refinement details of the X-ray diffraction data for In12 and In13 in *P1*

| | In12 | In13 |
|--------------------------|--|--|
| Lattice parameter | a=6.0578(3) Å, b=6.0644 (3)Å, c=6.0627(3)Å, α =60.33(1) $^\circ$, β =59.75(2) $^\circ$, γ =60.02(2) $^\circ$ | a=6.0540(1)Å, b=6.0671(3)Å, c=6.0624(2)Å, α =60.33(3) $^\circ$, β =59.74(2) $^\circ$, γ =60.03(1) $^\circ$ |
| Atom | x, y, z | x, y, z |
| Ba1 ^a | 0.2480(1), 0.2643(1), 0.2461(1) | 0.2432(1), 0.2620(2), 0.2531(1) |
| Ba2 ^a | 0.7451(3), 0.7663(3), 0.7491(3) | 0.7424(3), 0.7649(3), 0.7516(3) |
| Bi1/Pb1/In1 ^b | 0.0000, 0.0000, 0.0000 | 0.0000, 0.0000, 0.0000 |
| Bi2/Pb2/In2 ^b | 0.5054(2), 0.4951(2), 0.5024(2) | 0.5066(2), 0.4976(2), 0.5017(2) |
| O1 ^c | 0.2312(1), -0.7361(3), 0.6817(3) | 0.2164(1), -0.7153(3), 0.6869(3) |
| O2 ^c | 0.8489(3), 0.6158(2), 0.2456(1) | 0.8522(3), 0.6219(2), 0.2503(1) |
| O3 ^c | 0.7311(3), 0.2577(1), 0.2309(1) | 0.7518(3), 0.2503(1), 0.2171(1) |
| O4 ^c | 0.2215(1), 0.7544(3), 0.7307(3) | 0.2475(1), 0.7424(3), 0.7191(3) |
| O5 ^c | 0.2059(1), 0.7568(3), 0.3134(2) | 0.2193(1), 0.7594(3), 0.2976(2) |
| O6 ^c | 0.7289(3), 0.2351(1), 0.8080(3) | 0.7476(3), 0.2334(1), 0.7971(3) |
| R factor ^d | R _{wp} =0.0455, R _p =0.0313 | R _{wp} =0.0452, R _p =0.0300 |

^aThe occupancies of Ba1 and Ba2 are 1.0000 for In12 and In13.

^bThe occupancies of Bi1/Pb1/In1 and Bi2/Pb2/In2 are 0.22/0.66/0.1200 for In12, 0.2150/0.6450/0.1400 for In13.

^cThe occupancies of O1, O2, O3, O4, O5, and O6 are 1.0000, 1.0000, 1.0000, 1.0000, 1.0000 for In12 and In13.

dR_p is sum($|I_0 - I_C|$)/sum(I_0), and R_{wp} is weighted R factors for X-ray diffraction data.

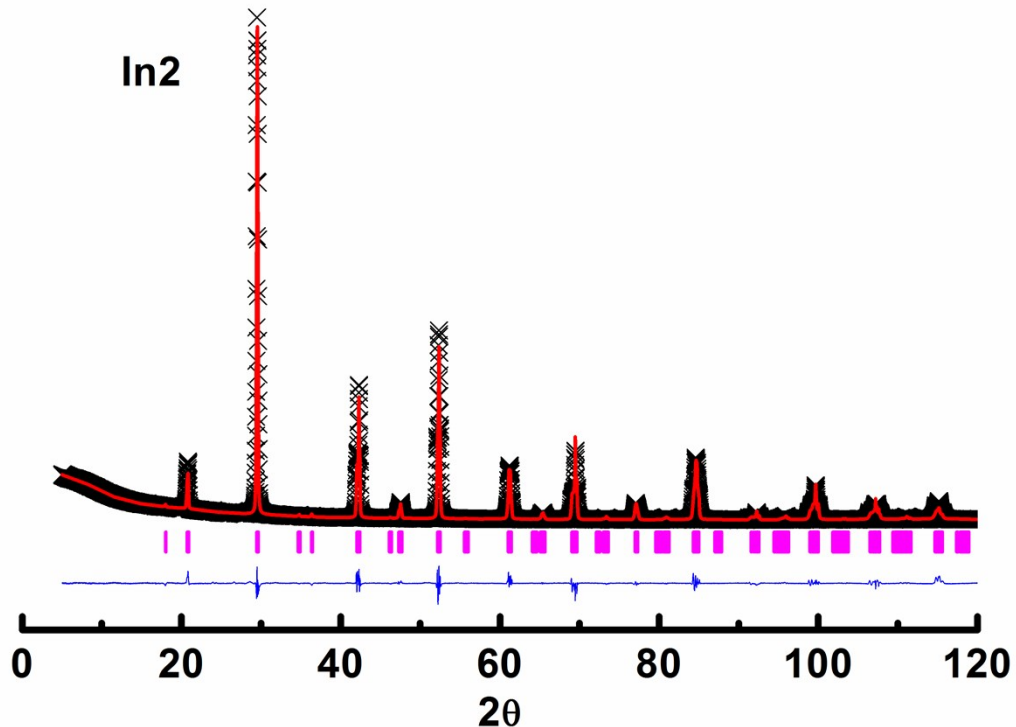


Figure S1 Rietveld plots of powder X-ray diffraction patterns ($\lambda_1=1.5405 \text{ \AA}$ and $\lambda_2=1.5443 \text{ \AA}$) for In2 at room temperature. The plus symbol represents the observed value, the solid line represents the calculated value, the marks below the diffraction patterns are the calculated reflection positions, and the difference curve is shown at the bottom in the figure.

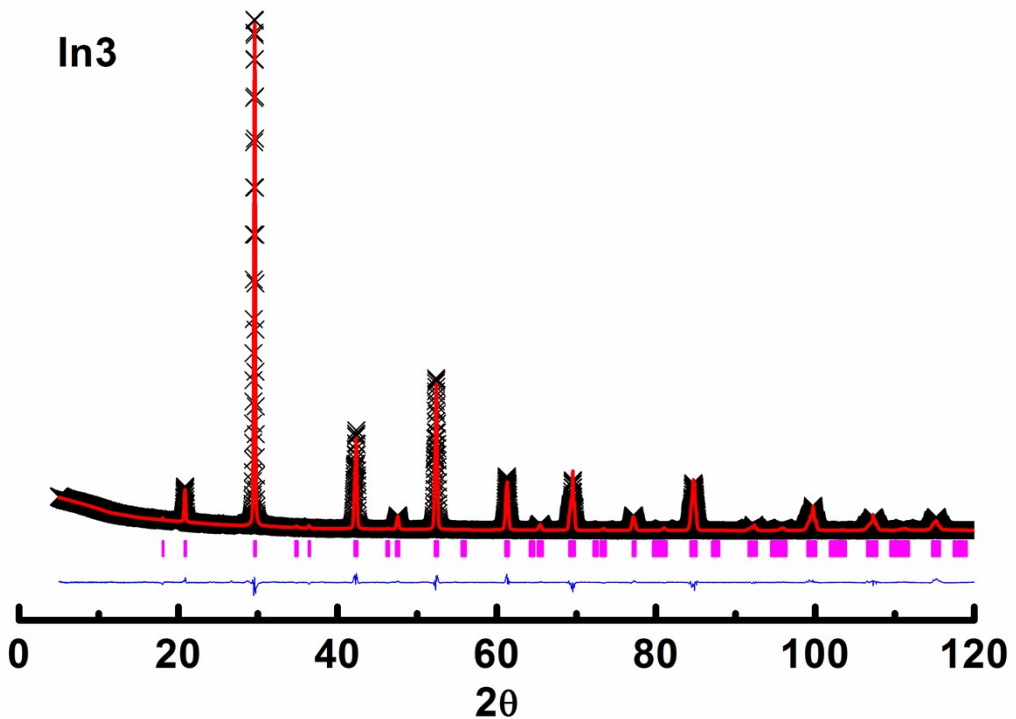


Figure S2 Rietveld plots of powder X-ray diffraction patterns ($\lambda_1=1.5405 \text{ \AA}$ and $\lambda_2=1.5443 \text{ \AA}$) for In3 at room temperature. The plus symbol represents the observed value, the solid line represents the calculated value, the marks below the diffraction patterns are the calculated reflection positions, and the difference curve is shown at the bottom in the figure.

curve is shown at the bottom in the figure.

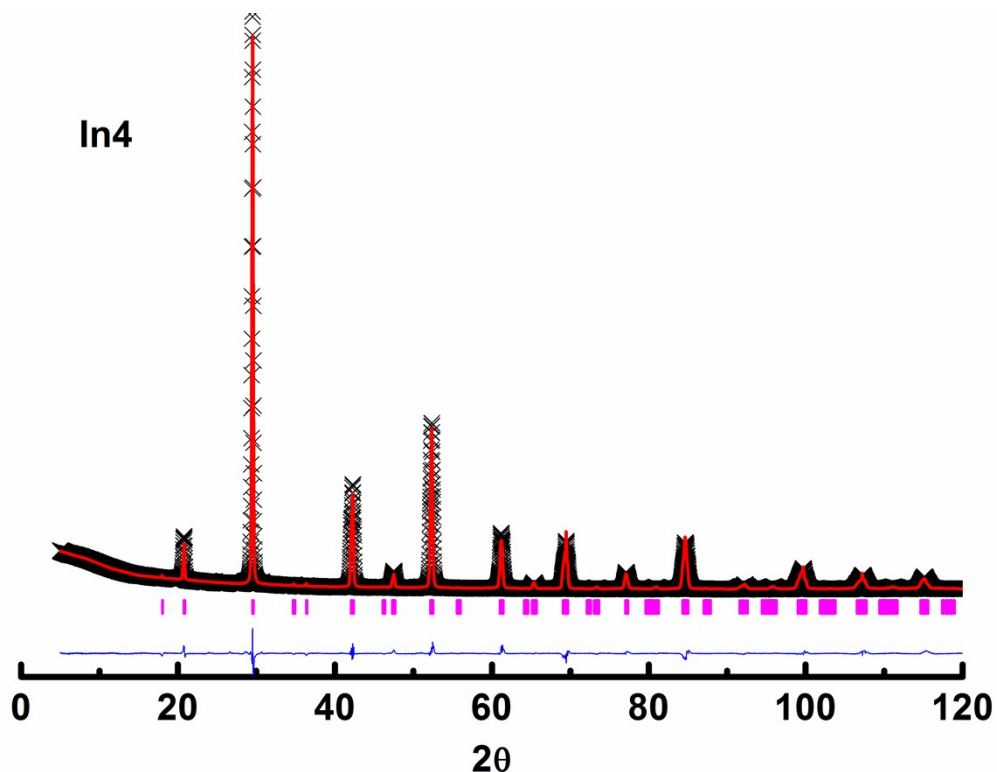


Figure S3 Rietveld plots of powder X-ray diffraction patterns ($\lambda_1=1.5405 \text{ \AA}$ and $\lambda_2=1.5443 \text{ \AA}$) for In4 at room temperature. The plus symbol represents the observed value, the solid line represents the calculated value, the marks below the diffraction patterns are the calculated reflection positions, and the difference curve is shown at the bottom in the figure.

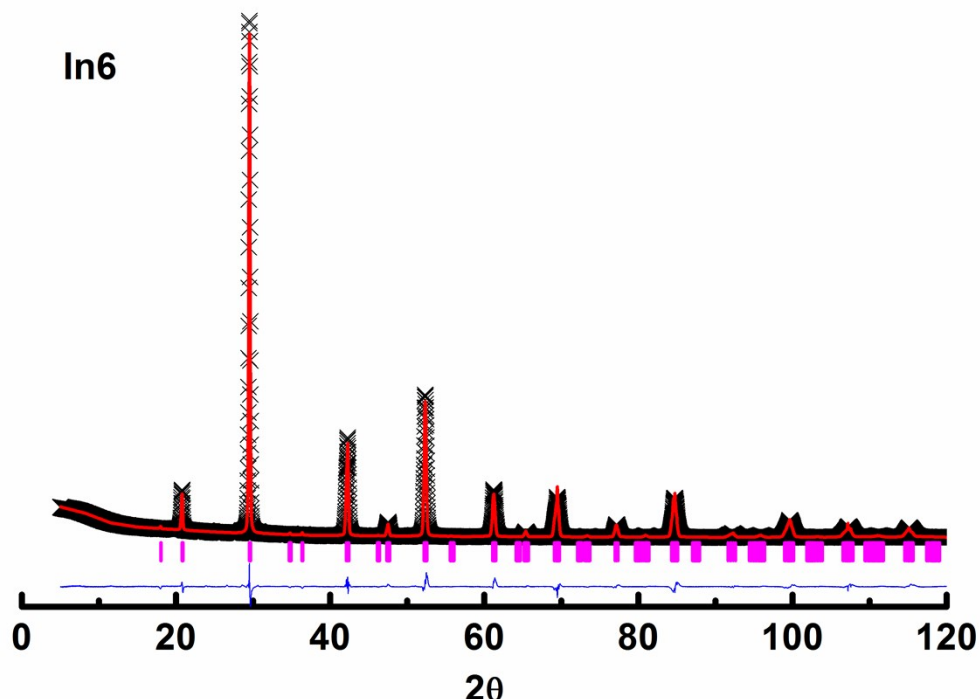


Figure S4 Rietveld plots of powder X-ray diffraction patterns ($\lambda_1=1.5405 \text{ \AA}$ and $\lambda_2=1.5443 \text{ \AA}$) for In6 at room temperature. The plus symbol represents the observed value, the solid line represents the

calculated value, the marks below the diffraction patterns are the calculated reflection positions, and the difference curve is shown at the bottom in the figure.

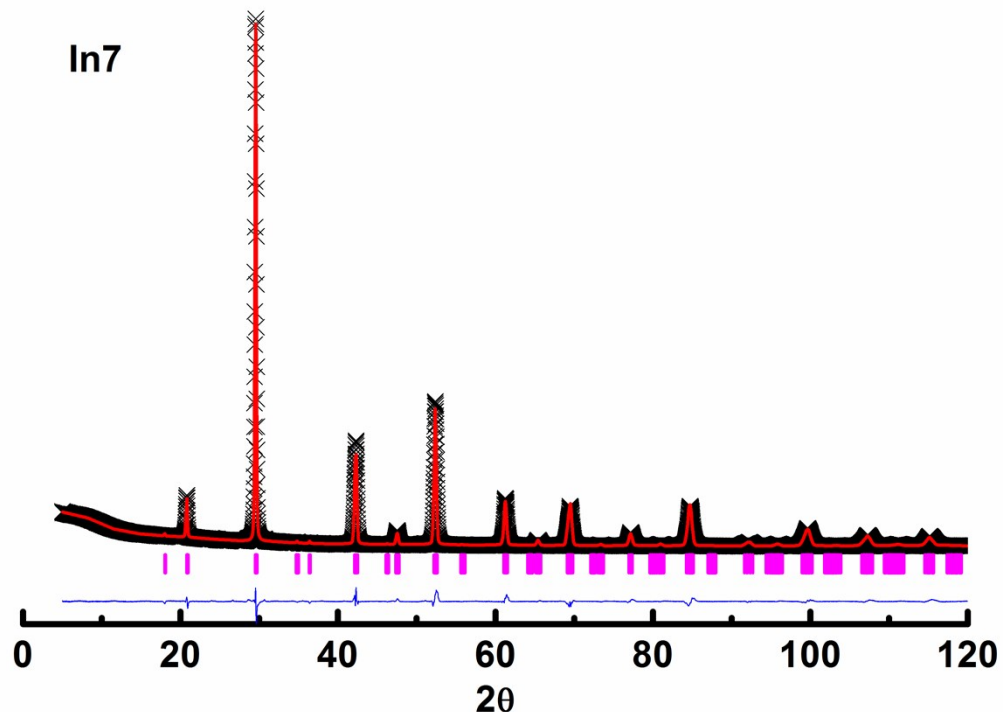


Figure S5. Rietveld plots of powder X-ray diffraction patterns ($\lambda_1=1.5405$ Å and $\lambda_2=1.5443$ Å) for In7 at room temperature. The plus symbol represents the observed value, the solid line represents the calculated value, the marks below the diffraction patterns are the calculated reflection positions, and the difference curve is shown at the bottom in the figure.

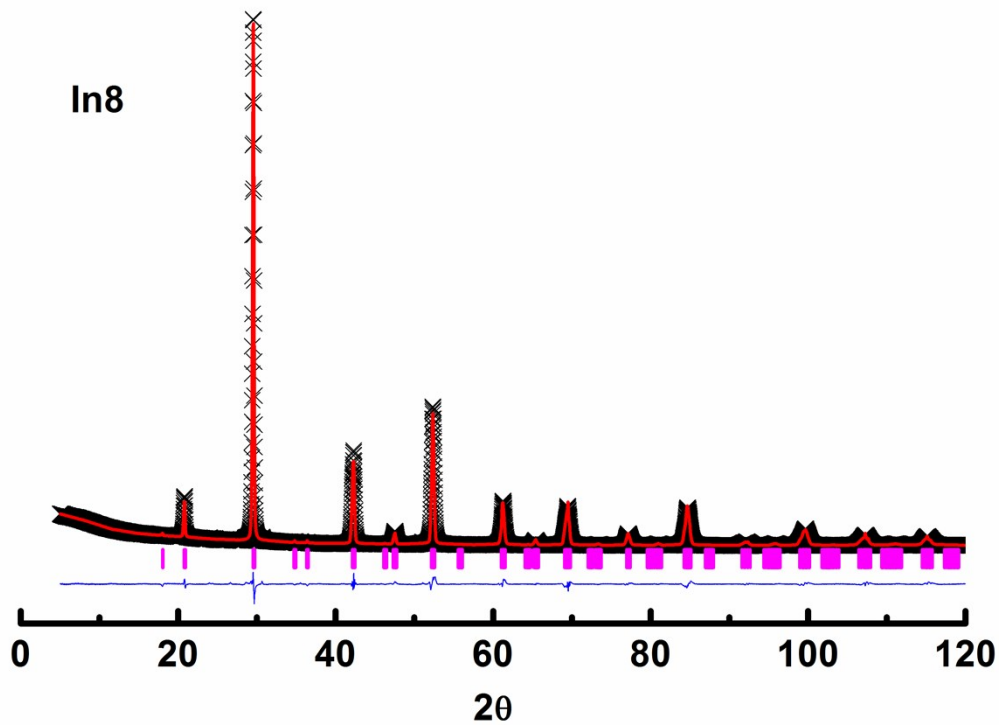


Figure S6 Rietveld plots of powder X-ray diffraction patterns ($\lambda_1=1.5405$ Å and $\lambda_2=1.5443$ Å) for In8 at

room temperature. The plus symbol represents the observed value, the solid line represents the calculated value, the marks below the diffraction patterns are the calculated reflection positions, and the difference curve is shown at the bottom in the figure.

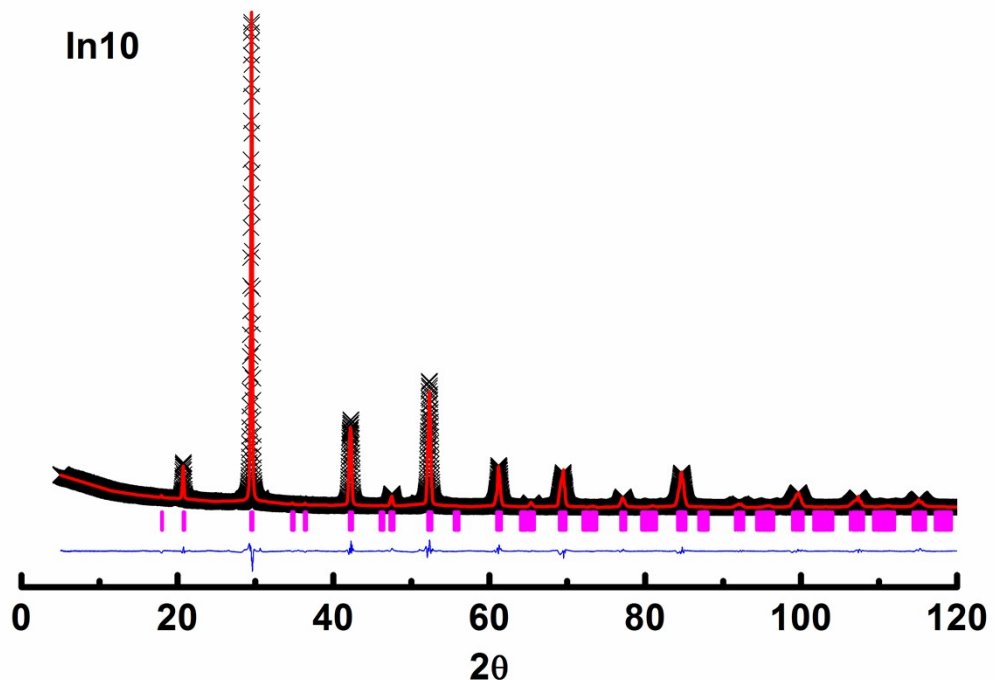


Figure S7 Rietveld plots of powder X-ray diffraction patterns ($\lambda_1=1.5405 \text{ \AA}$ and $\lambda_2=1.5443 \text{ \AA}$) for In10 at room temperature. The plus symbol represents the observed value, the solid line represents the calculated value, the marks below the diffraction patterns are the calculated reflection positions, and the difference curve is shown at the bottom in the figure.

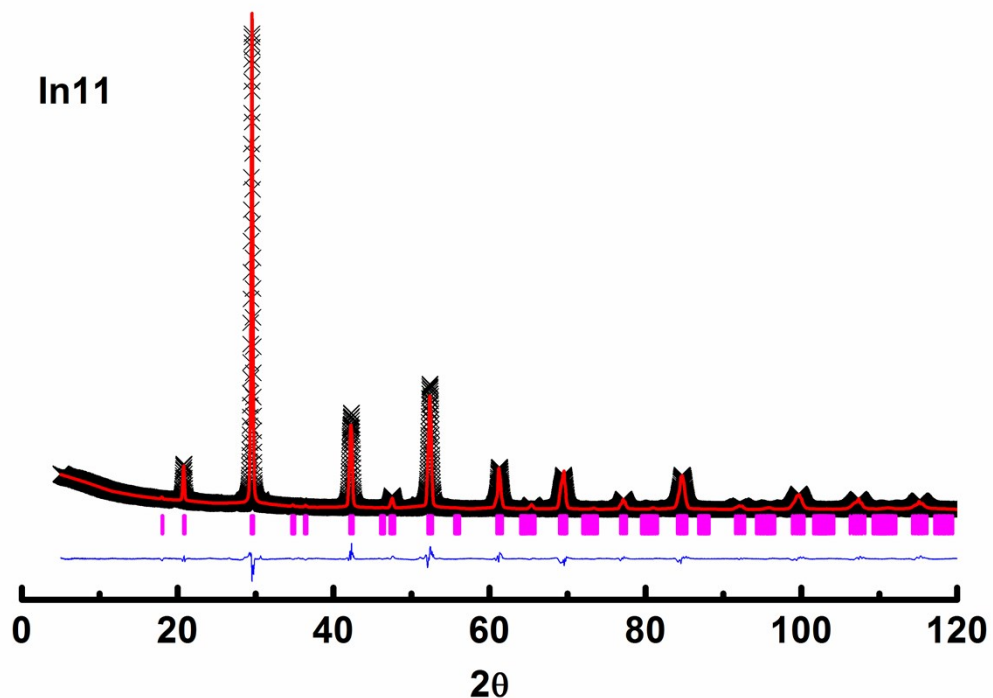


Figure S8 Rietveld plots of powder X-ray diffraction patterns ($\lambda_1=1.5405 \text{ \AA}$ and $\lambda_2=1.5443 \text{ \AA}$) for In11 at room temperature. The plus symbol represents the observed value, the solid line represents the calculated value, the marks below the diffraction patterns are the calculated reflection positions, and the

difference curve is shown at the bottom in the figure.

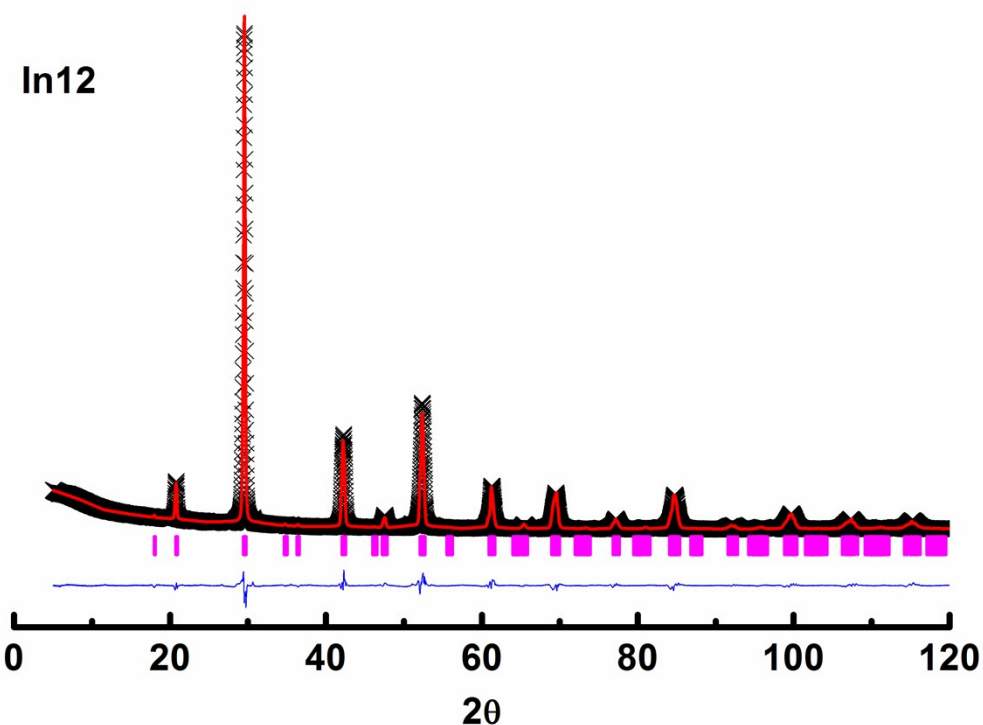


Figure S9 Rietveld plots of powder X-ray diffraction patterns ($\lambda_1=1.5405 \text{ \AA}$ and $\lambda_2=1.5443 \text{ \AA}$) for In12 at room temperature. The plus symbol represents the observed value, the solid line represents the calculated value, the marks below the diffraction patterns are the calculated reflection positions, and the difference curve is shown at the bottom in the figure.

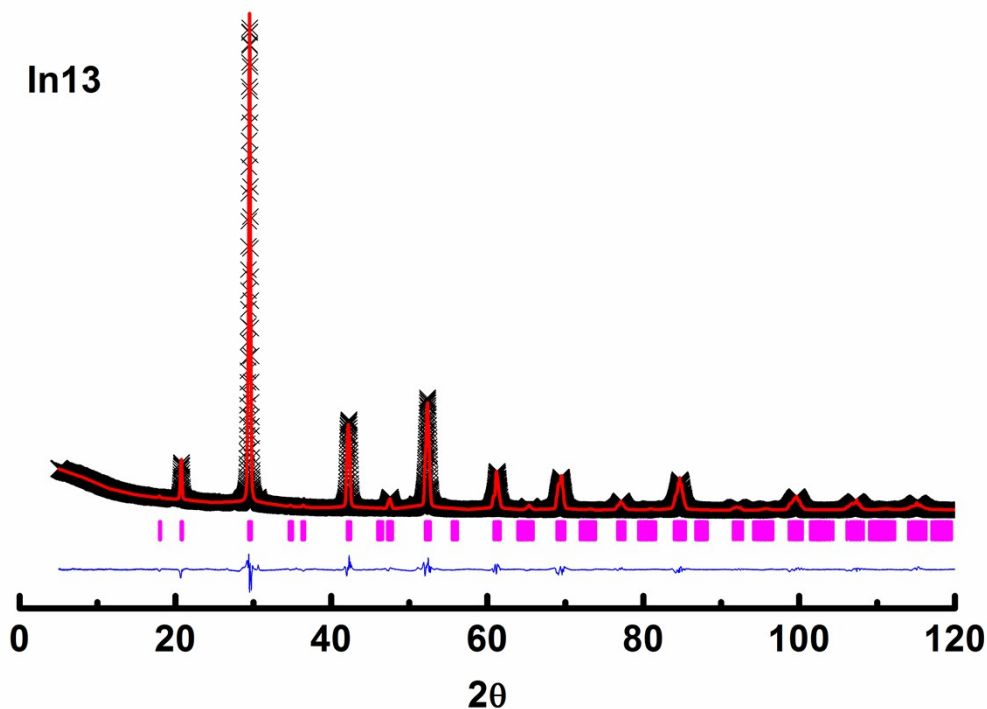


Figure S10 Rietveld plots of powder X-ray diffraction patterns ($\lambda_1=1.5405 \text{ \AA}$ and $\lambda_2=1.5443 \text{ \AA}$) for In13 at room temperature. The plus symbol represents the observed value, the solid line represents the calculated value, the marks below the diffraction patterns are the calculated reflection positions, and the difference curve is shown at the bottom in the figure.

3. Temperature-dependent resistance of $\text{Ba}(\text{Bi}_{0.25}\text{Pb}_{0.75})_{1-x}\text{In}_x\text{O}_{3-\delta}$

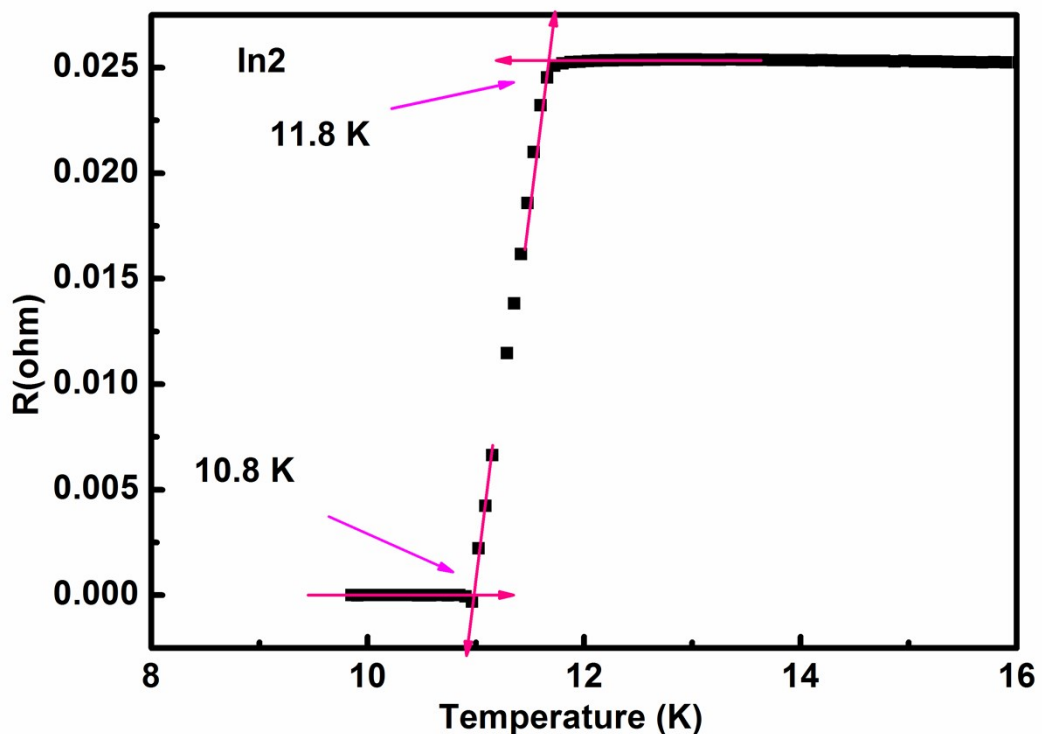


Figure S11 Temperature-dependent resistance of In2.

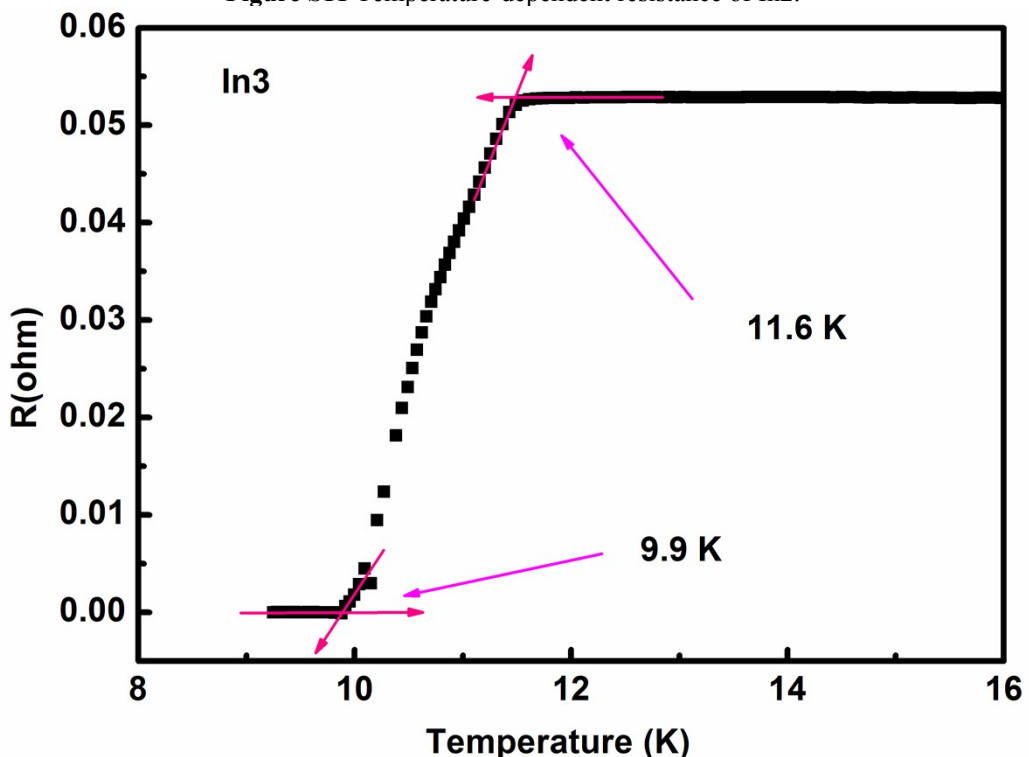


Figure S12 Temperature-dependent resistance of In3.

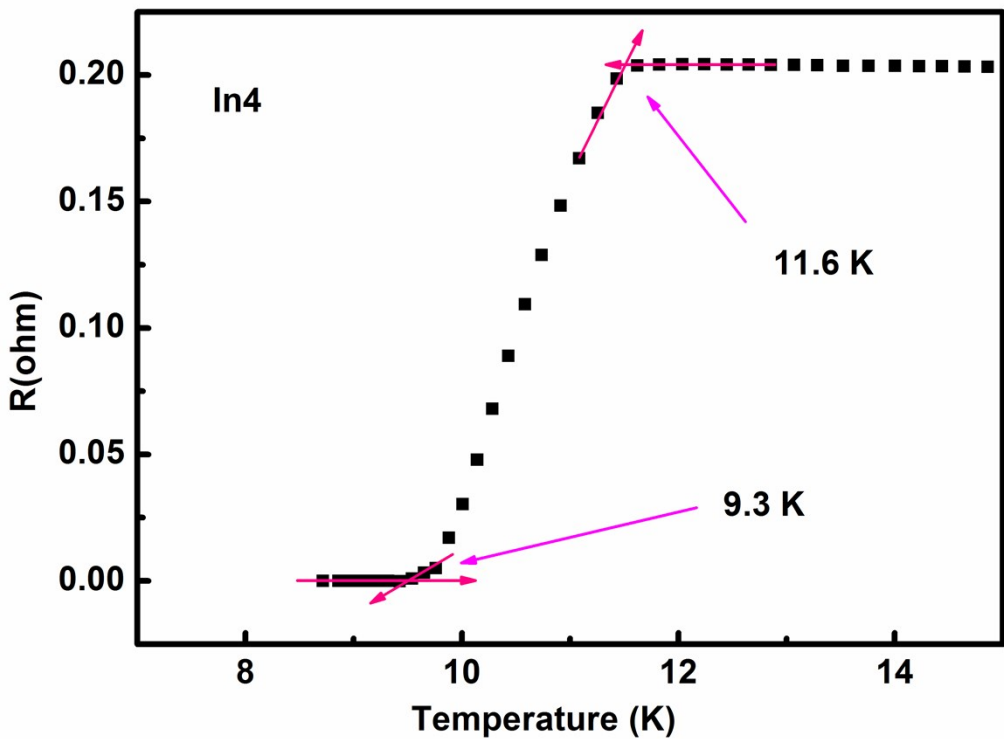


Figure S13 Temperature-dependent resistance of In4.

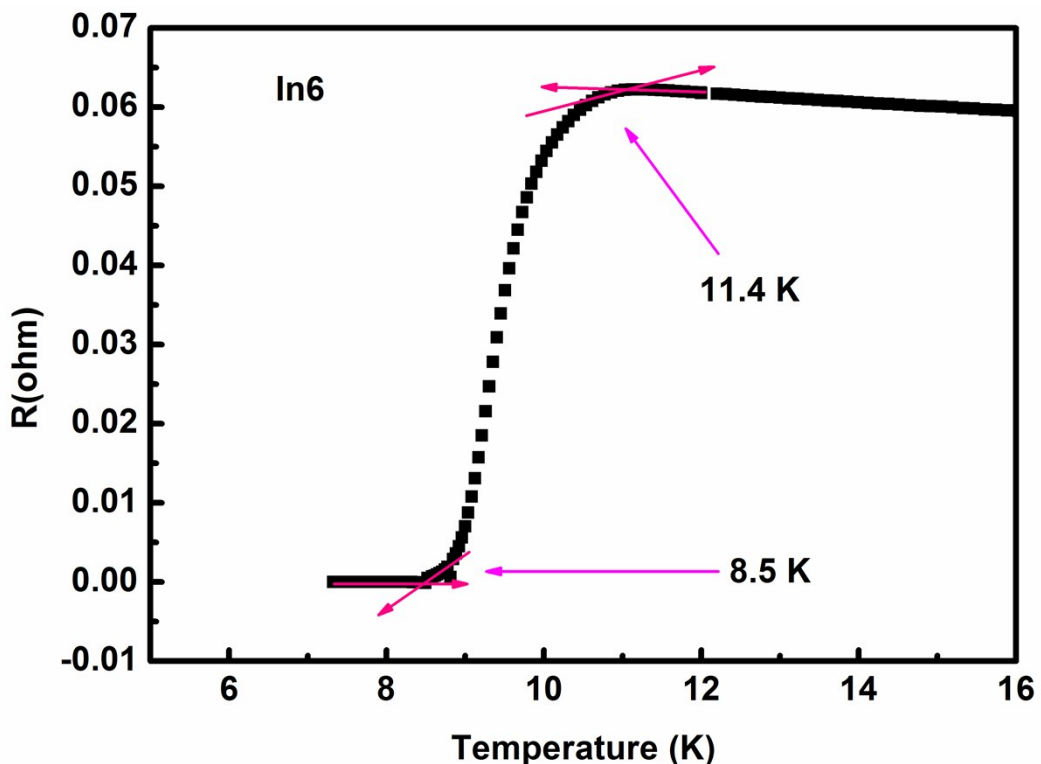


Figure S14 Temperature-dependent resistance of In6.

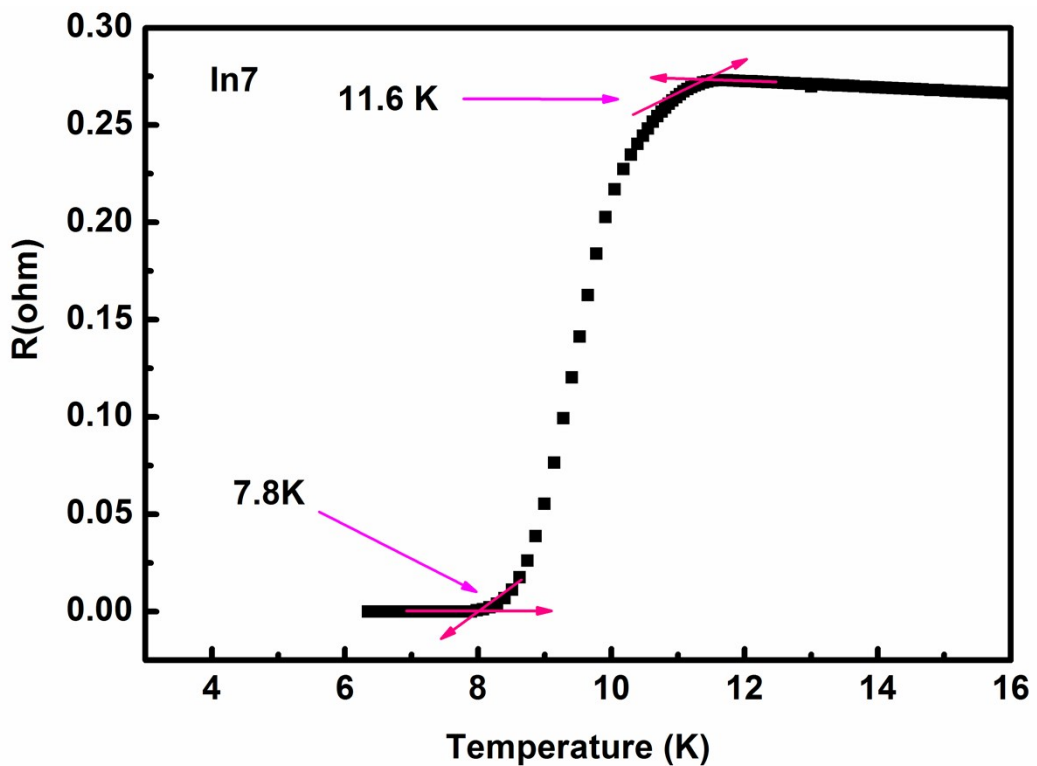


Figure S15 Temperature-dependent resistance of In7.

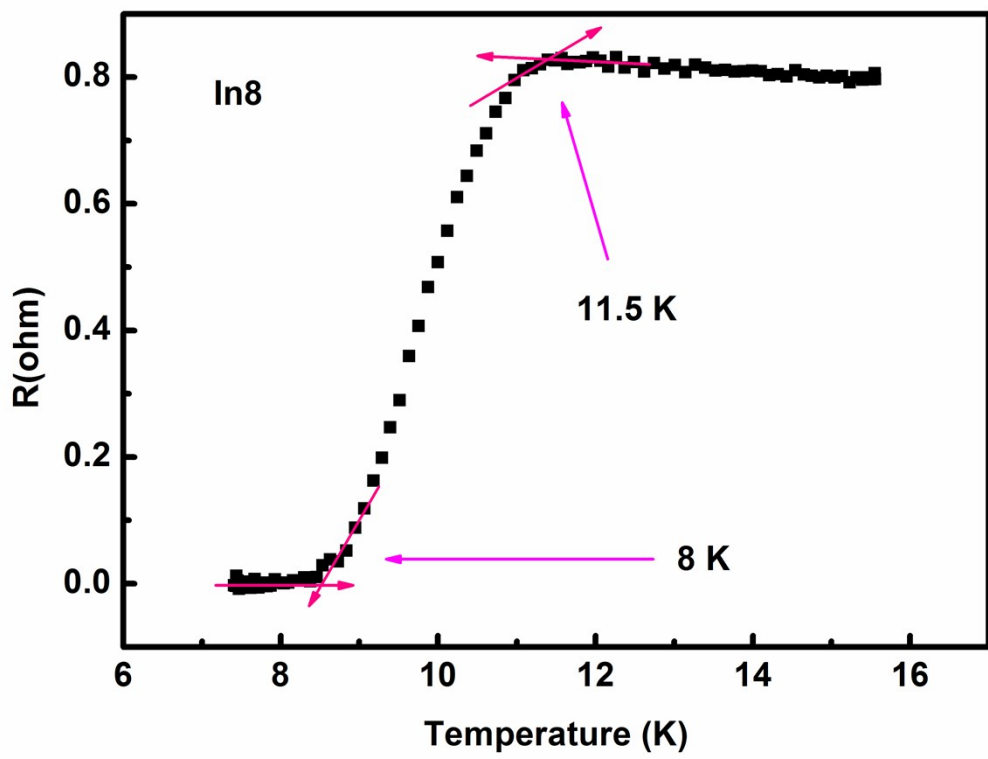


Figure S16 Temperature-dependent resistance of In8.

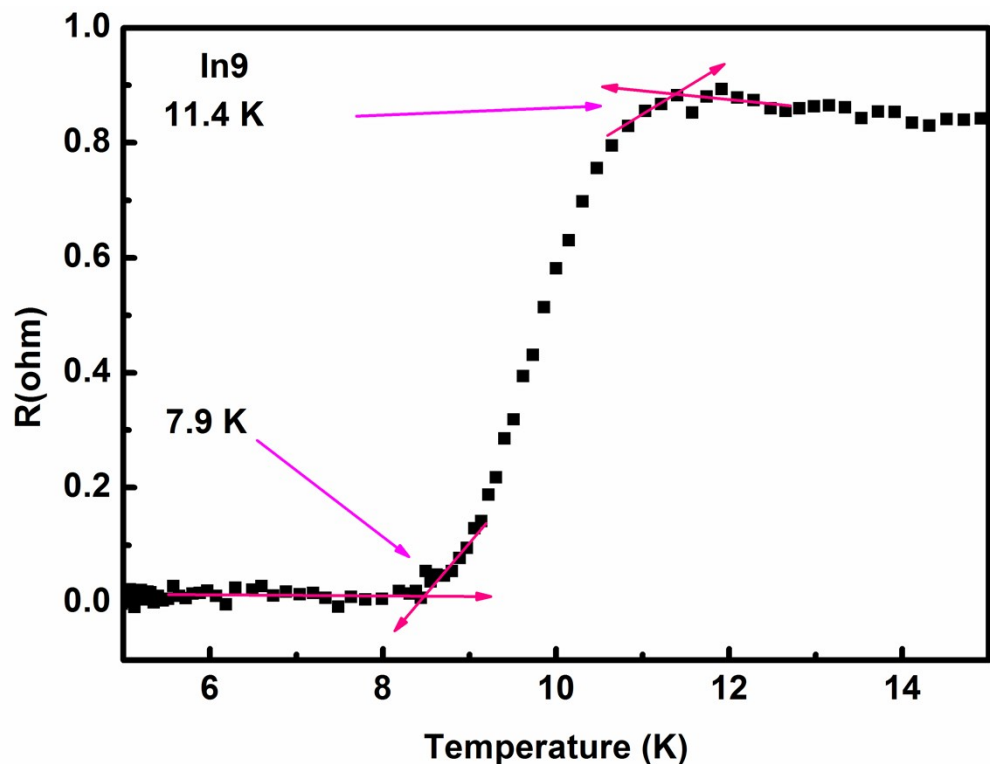


Figure S17 Temperature-dependent resistance of In9.

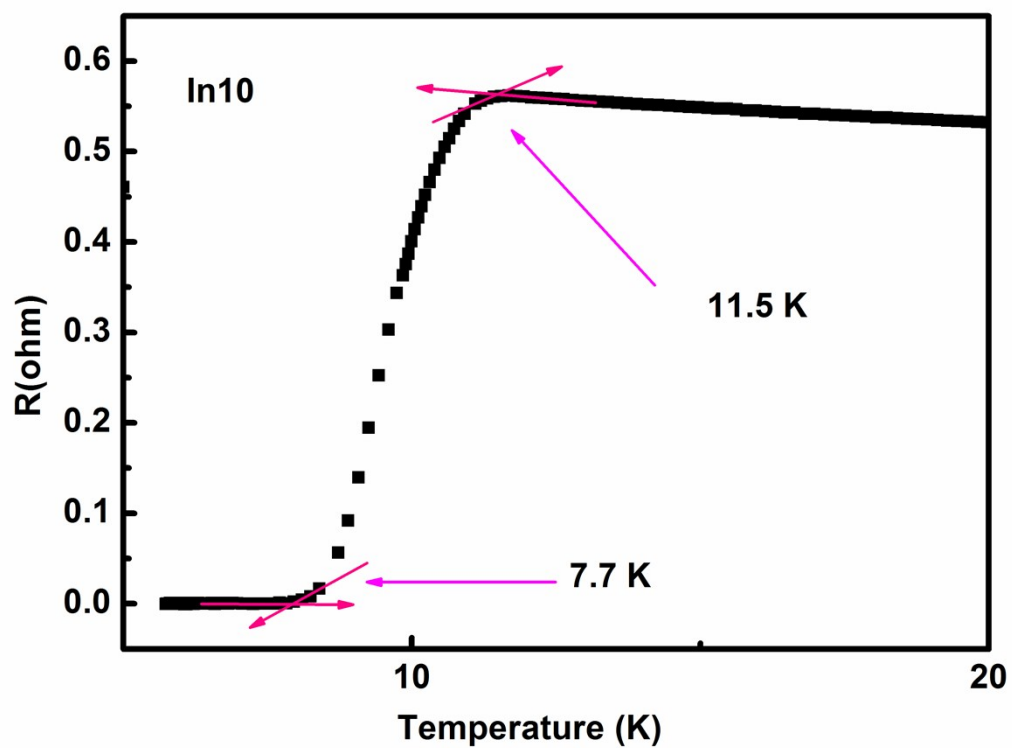


Figure S18 Temperature-dependent resistance of In10.

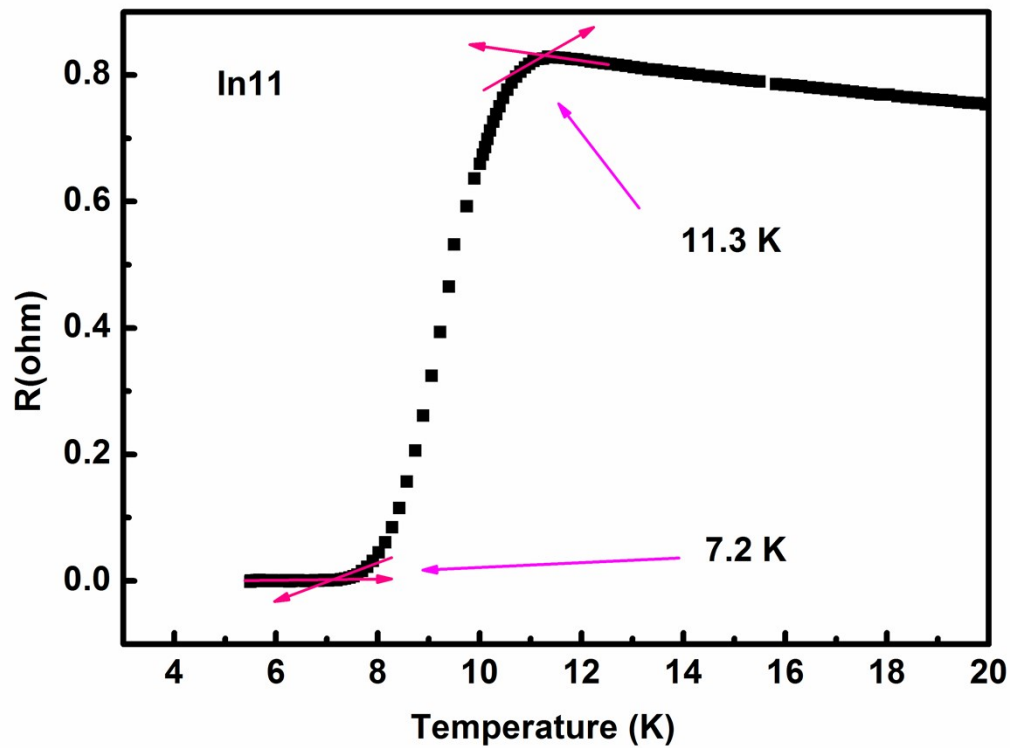


Figure S19 Temperature-dependent resistance of In11.

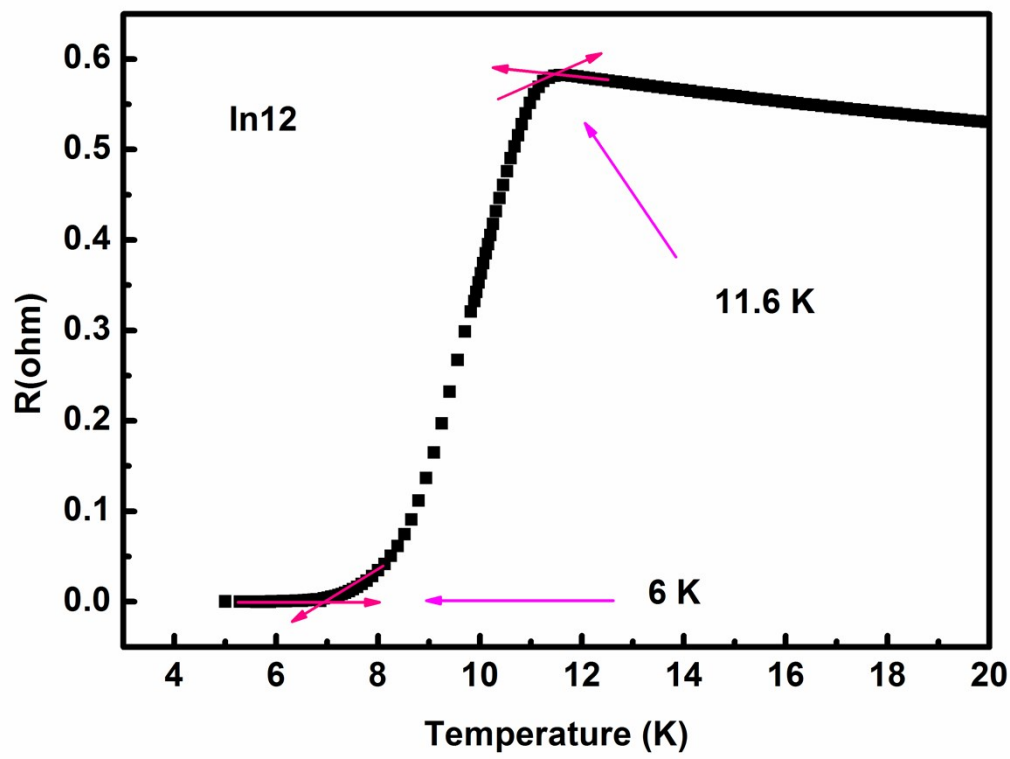


Figure S20 Temperature-dependent resistance of In12.